ELSEVIER

International Journal of Mass Spectrometry 206 (2001) 267–273

International Journal of Mass Spectrometry

Multipass time-of-flight mass spectrometers with high resolving powers

A. Casares, A. Kholomeev, H. Wollnik

Justus-Liebig-University, 35392 Giessen, Germany

Received 8 June 2000; accepted 4 October 2000

Abstract

Low energy ions can be stored in "rings" of electrostatic sector fields or in systems of electrostatic mirrors between which the ions are reflected back and forth repeatedly. Because of the long flight path in such systems they very well can be used as precision time-of-flight mass spectrometers. This statement is trivial for monoenergetic ions but also holds for polyenergetic ions if the ion–optical system is designed such that it guides more energetic ions on appropriate detours that cause the overall ion-travel times to become energy independent. Since the number of reflections between the mirrors can be varied by changing the timing of the voltage pulses on the mirrors, either a long well resolved mass spectrum can be recorded or only a section of such a mass spectrum for which then the mass resolving power is increased proportional to the number of reflections. (Int J Mass Spectrom 206 (2001) 267–273) © 2001 Elsevier Science B.V.

Keywords: Time-of-flight mass spectrometers; High mass resolving power

1. Introduction

Energetic ions can be kept circulating for an extended period of time in a ring of sector fields and interspersed straight-axis lenses. Alternatively they can be reflected back and forth between ion mirrors. In both such systems the diameters of an ion beam can be kept small with the beam envelope going through maxima and minima [1] that usually differ only by a small factor, for instance of 2. Since both systems are characterized by a long flight path, they can very well be used as multipass time-of-flight mass spectrometers (MTOF-MSs). There are three such systems used so far. (1) high-energy storage rings in which monoenergetic ions circulate so that the flight times per turn reveal the ion masses [2,3]; (2) high- and low-energy storage rings in which polyenergetic ions circulate such that the more energetic ones move along detours so that the systems are energy isochronous, i.e. their flight times per turn do not depend on the ion energies though they still vary with the ion masses [1,4–9]; (3) low-energy systems in which polyenergetic ions are repeatedly reflected between electrostatic ion mirrors such that the more energetic ions penetrate deeper into the repeller fields of the ion mirrors. Thus the systems can also be energy isochronous [4,7,10–12].

2. Ion optics for multipass TOF-MS systems

Storage rings as well as multipass mirror systems are best designed as a multitude of equal "cells" with

* Corresponding author. E-mail: h.wollnik@uni-giessen.de.

PII S1387-3806(00)00391-2

beam waists at their entrances and their exits. Each cell has a curvilinear optic axis, the z axis, with planes that are perpendicular to this z axis at the cell entrance, $z = z_i$, and at the cell exit, $z = z_{i+1}$ being assumed to be equipotential planes.

Let us look now at one half of a "cell" and assume that we have only singly charged ions in the beam and that we postulate (1) a reference ion that when starting at $z = z_i$, has the mass m_0, energy K_0 and momentum p_0 and moves along the curvilinear z axis from the cell entrance at $z = z_i$ to the half cell plane at $z = z_{i+1}$ in a time t_0 and (2) an arbitrary ion that when starting at $z = z_i$ has the mass $m = m_0(1 + \delta_m)$, energy $K(z_i) = K_0(1 + \delta_K)$ and momentum $p(z_i) = p_0(1 + \delta_p)$. This ion moves from the cell entrance at $z = z_i$ to the cell middle $z = z_{i+1}$ in a time $t_0[1 + \delta_t]$. Here it is assumed that the ion had started at $z = z_i$ a lateral distance "$x_i = x(z_i)$" away from the optic axis under an inclination "$a_i = a(z_i) = p_x(z_i)/p_0$" and reached a final lateral ion position "$x(z_i+1)$" under an inclination "$a(z_i+1) = p_x(z_{i+1})/p_0$."

In a first-order approximation one describes the ion motion by the system transfer matrix for the first half of a cell as

$$\begin{pmatrix} x_{i+1} \\ a_{i+1} \\ \delta_K \\ \delta_t \end{pmatrix} = \begin{pmatrix} (x|x) & (x|a) & (x|\delta_K) & 0 \\ (a|x) & (a|a) & (a|\delta_K) & 0 \\ 0 & 0 & 1 & 0 \\ (t|x) & (t|a) & (t|\delta_K) & 1 \end{pmatrix} \begin{pmatrix} x_i \\ a_i \\ \delta_K \\ 0 \end{pmatrix} \quad (1)$$

Passing an ion through a full symmetric cell, i.e. the second "half cell" is the reverse of the first half cell, the total transfer matrix reads from $z = z_i$ to $z = z_{i+2}$

$$\begin{pmatrix} 2(x|x)(a|a) - 1 & 2(a|a)(x|a) & 2(x|a)(a|\delta_K) & 0 \\ 2(x|x)(a|x) & 2(x|x)(a|a) - 1 & 2(x|x)(a|\delta_K) & 0 \\ 0 & 0 & 1 & 0 \\ -2(x|x)(a|\delta_K) & -2(x|a)(a|\delta_K) & 2[(t|\delta_K) - (x|\delta_K)(a|\delta_K)] & 1 \end{pmatrix} \quad (2)$$

Choosing the parameters of the cell such that Eq. (2) becomes a unity matrix, one certainly has a good solution for a multipass time-of-flight mass spectrometer. In this case the product of N such unity matrices will cause any ion trajectory to leave the cell at the same position and with the same inclination as the incoming trajectory was characterized by. As one sees from Eq. (2) this condition is achieved if

$$(x|x) = (a|a) = 0 \quad (3)$$

$$(a|\delta_K) = (t|\delta_K) = 0 \quad (4)$$

3. Design and operation of a MTOF-MS

It was our goal to build a high performance energy-isochronous multipass time-of-flight mass spectrometer by using not a storage ring but a multireflection device employing electrostatic ion mirrors. Such systems have been built, e.g. (1) in [11] with an electron impact storage ion source [14] and relatively difficult to control grid-free ion mirrors, and (2) in [15] with a matrix-assisted laser desorption ionization (MALDI) ion source and gridded ion mirrors that have a reduced ion transmission.

3.1. Geometry of the MTOF-MS

We have now built a new system that uses an electron impact storage ion source in which ions are produced continuously, stored in some potential well formed by the electron beam and released every 500 or 1000 μs. This release is performed such that at the end an ion pulse of a few nanosecond length is generated [14] as was the case in the MTOF-MS of [11].

To achieve an overall improved performance for the new MTOF-MS we changed the V-shaped ion path used in [11] into a U-shaped [12] one (see Fig. 1) which allowed a more precise mechanical mounting of our mirror arrangement. Such a precise mounting of the different mirrors is important for a system that uses grid-free ion mirrors since already small beam shifts will send the ion beam through different parts of

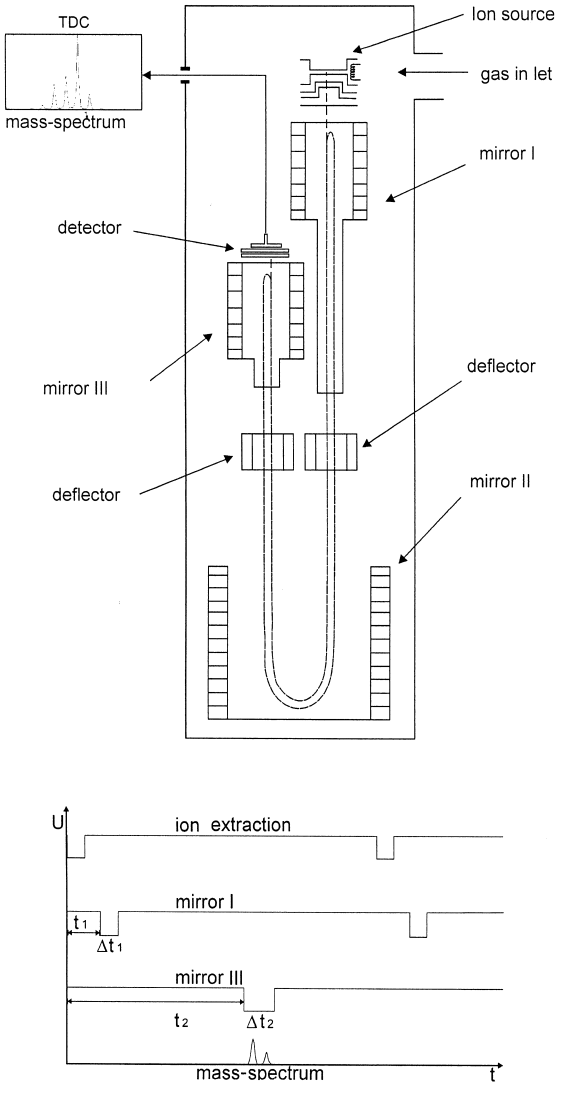

Fig. 1. Geometry of the built time-of-flight mass spectrometer is shown together with the time variations of the voltages on the ion mirrors I and III. Note here that the Δt_1 long pulse on mirror I is delayed by a variable time t_1 with respect to the short ion source extraction pulse. Thus only such ions can enter the race track whose flight time from the ion source to mirror I is between t_1 and $t_1 + \Delta t_1$. This allows to eliminate too light $m \leq m_1$ and too heavy $m \geq m_2$ ions. Note also the geometrical arrangement of the static mirror II, that has an inner diameter of 59 or 70 mm, and the switchable mirrors I and III of both 40 mm, respectively. The shown beam deflectors are only used to compensate mechanical alignment errors and ideally are switched off completely.

the inhomogeneous fringing field of the ion mirror. Very important were also theoretical numerical calculations in which we varied the electrode geometry again and again determining in each case the magnitude of the elements of the transfer matrix $(x|x)$, $(a|a)$, $(a|\delta_K)$, and $(t|\delta_K)$ by ray tracing calculations. In these calculations we obtained at the end very small values of these matrix elements. The overall ion paths are shown in Fig. 2 together with the potential distributions which illustrate the action of an accelerating Einzel lens. Also shown is the intermediate lateral image in the turn around point of the static ion mirror. The location of this intermediate image ensures a laterally dispersion-free system [1] which is important for such a long overall flight path. Though all these conditions were fulfilled in theoretical calculations, experimentally we could only measure the overall achieved isochronicity and the system transmission.

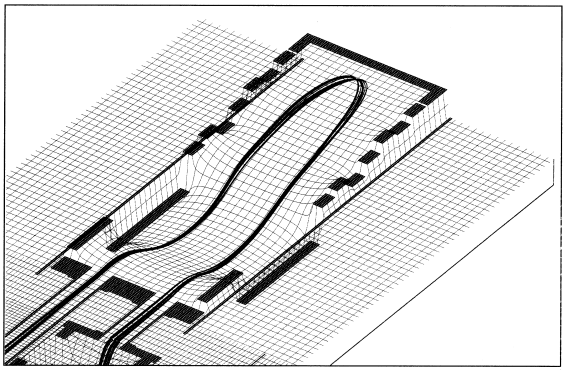

Fig. 2. Ion trajectories in the main part of the MTOF-MS of Fig. 1 are shown as a computer simulation by SIMION V6. This simulation shows the ion trajectories as they pass through the potential distribution of the MTOF-MS for a multipass situation.

3.2. Potentials of the electrodes

In a multireflection time-of-flight mass spectrometer the overall beam path is divided into the repetitive cell arrangement through which the ion beam passes multiple times and the entrance and exit optics. These entrance and exit optics require that the potentials of the electrodes in mirror I and mirror III of Fig. 1 are intermittently reduced to allow the ion beam to enter and to leave the system. A timing diagram that shows when the mirrors I and III transmit or reflect ions is

given in Fig. 1. In order that (1) the ions can reach the final ion detector after they have passed through the MTOF-MS, the ion mirror 3 is opened for a time Δt_2 starting a time t_2 after the formation of an ion bunch in the ion source. Here t_2 and $t_2 + \Delta t_2$ are those times that ions of masses $m_1 = m_0 - \Delta m$ and $m_2 = m_0 + \Delta m$ would need to perform $2N + 1$ passages, respectively, and (2) the ions can enter the MTOF-MS, the ion mirror 1 is opened for a time Δt_1 starting a time t_1 after the formation of an ion bunch. Since the lighter ions move through the distance between the ion source and the back of mirror 1 earlier than the heavier ones, one can achieve that for a proper choice of t_1 and Δt_1 only ions in the mass window $m_1 \leq m_0 \leq m_2$ can enter the "race track." Though this mass selection is not very precise this mass window can ensure that, when the ions of mass m_0 are released from the race track after $2N + 1$ passages, there are no ions that would have gone through $2N + 3$ or $2N - 1$ passages in the same time, i.e. $m \leq m_1$ or $m \leq m_2$.

4. Experimental results

The system we have built and tested uses three ion mirrors consisting of grid-free ring electrodes except for the final reflecting electrodes which do contain one grid. However, in the multireflection mode the potentials of the grids in these electrodes were chosen to be so high that the ions turned around before impacting on these grids. Only during entrance into and exit out of the system, i.e. when the electrode potentials of the switcheable mirrors were reduced, the ions had to pass once through the grids of the last electrodes of mirrors I and III. These passes caused intensity losses of ≈10% each, with these losses being independent of the number of passes of the ions along the multireflection path.

In detail we have built and tested two systems: (1) the MTOF-MS "S" had an overall system length of 0.4 m, a static ion mirror of inner diameter 59 mm and two switched ion mirrors of inner diameters of 40 mm. This system achieved a single-pass mass resolv-

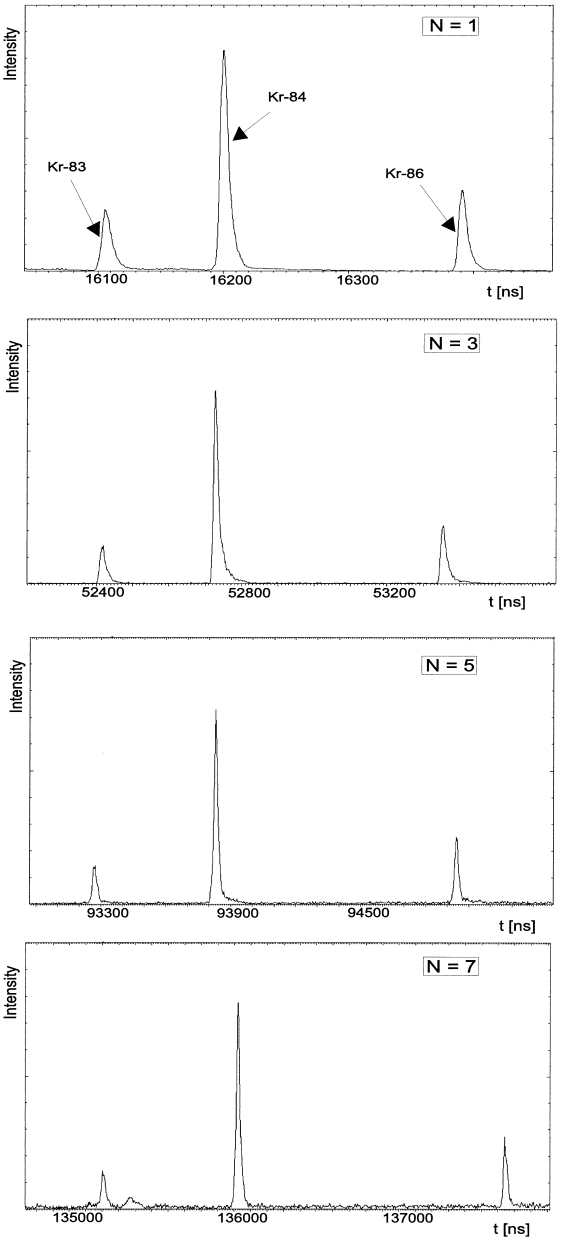

Fig. 3. Increase of the mass resolving power $R = m/\Delta m = t/2\Delta t$ in the 0.4 m long system S is illustrated by the mass spectrum of Kr as obtained for $N = 1, 3, 5, 7$ passes through the MTOF-MS. The corresponding flight times are for ^{84}Kr: 16.20, 52.75, 93.85, 136.0 μs and the FWHM peak widths 9.1, 17.2, 18.6, 22.5 ns with resulting mass resolving powers $R = m/\Delta m$ of 890, 1530, 2520, 3020.

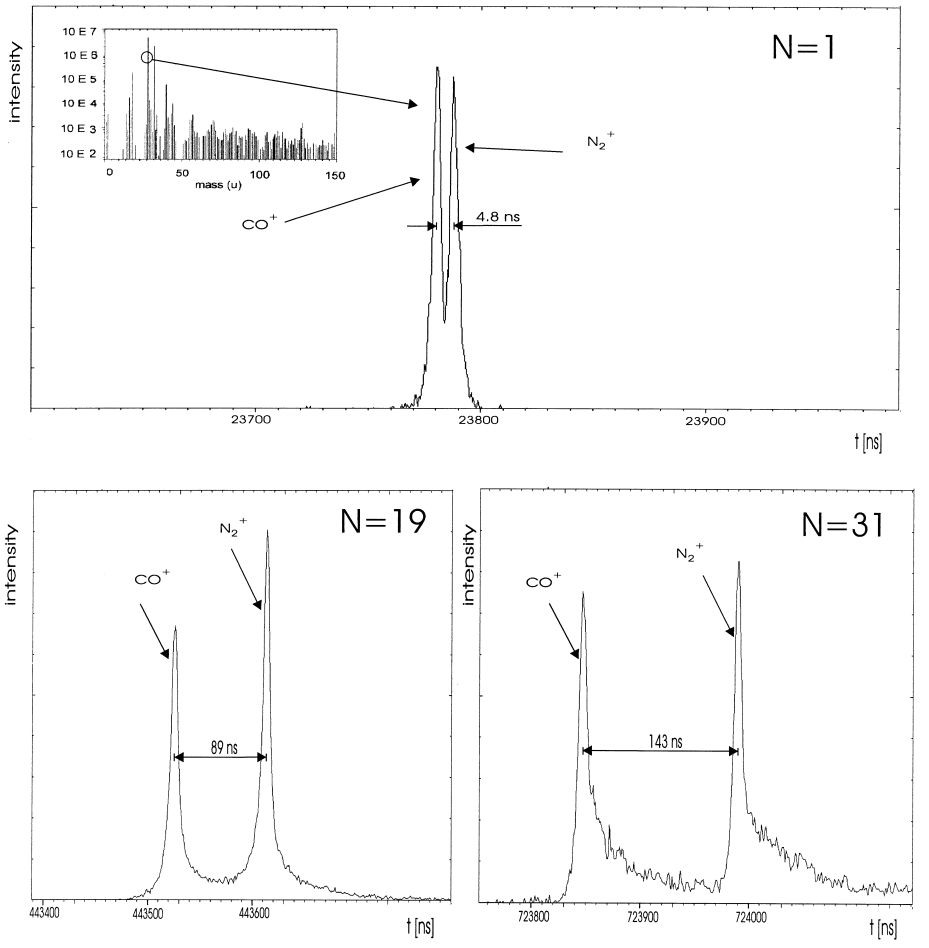

Fig. 4. Increase of the mass resolving power $R = m/\Delta m = t/2\Delta t$ in the 1.2 m long system L is illustrated by the mass spectrum of CO-enriched laboratory air as taken for $N = 1$, 19, 31 passes with special attention to the mass doublet of CO and N_2 ions which have mass values of 27.995 and 28.006 u. For $N = 31$ the mass difference of 0.011 u between the CO and N_2 ions thus could be measured with errors of $\leq 10^{-4}$ u or, which is the same, of $\leq$100 ke V.

ing power $m/\Delta m \approx 900$ (see Fig. 3, $N = 1$) and a 7-pass mass resolving power $m/\Delta m \approx 3000$ (see Fig. 3, $N = 7$), and (2) the MTOF-MS "L" had an overall system length of 1.2 m and a static ion mirror of an inner diameter of 70 mm and two switched ion mirrors of inner diameters of 40 mm. This system achieved a single-pass mass resolving power $m/\Delta m \approx 2900$ (see Fig. 4, $N = 1$) and a 19-pass mass resolving power $m/\Delta m \approx 24000$. In case of 31 passes through the system or a total flight path of $\approx$70 m even mass resolving powers $m/\Delta m \geq 50000$ were reached (see Fig. 4, $N = 31$).

In order to demonstrate that the mass resolving power $R = m/\Delta m$ increases with N the number of passes through the MTOF-MS mass spectra of Kr were recorded with the S system for $N = 1$, 3, 5, and 7 (see Fig. 3). As one can see the flight times and thus also the differences in the arrival times of the different ionized Kr isotopes increased linearly with N. The peak widths increased only slightly with N, however, so that also the mass resolving power $R = m/\Delta m$ increased approximately linear with N. For the same reason also the signal-to-noise ratio was approximately the same for all N values.

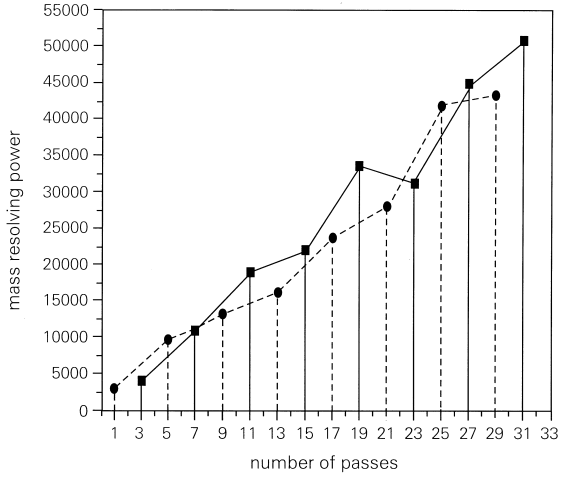

Fig. 5. For the MTOF-MS L the mass resolving power $R = m/\Delta m$ is plotted as function of N, the number of passes through the system. Note that R increases approximately linear with N. Note also that we have connected all points that correspond to $1 + 4K$ and $3 + 4K$ passes, respectively, since after 4 passes the image aberrations compensate to a large extent [6].

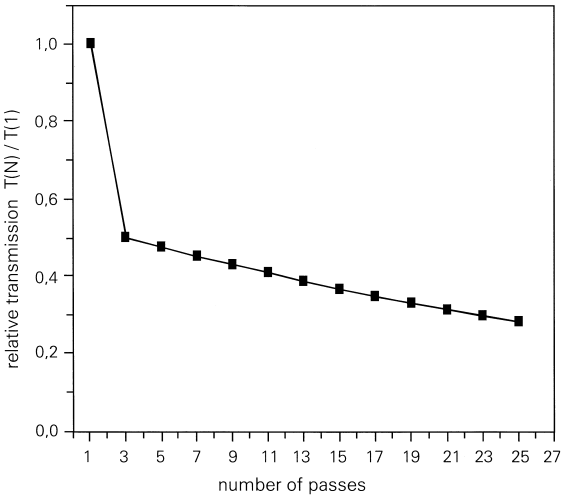

Fig. 6. For the MTOF-MS L the mass relative transmission $T(N)/T(N = 1)$ is plotted as function of N, the number of passes through the system. Note that N decreases by ≈50% between $N = 1$ and $N = 3$ and by ≈5% for every additional $2N$. After $N = 31$ passes thus a relative transmission of ≈25% was obtained.

In order to demonstrate that really high mass resolving powers can be reached in Fig. 4 mass spectra are shown of CO-enriched laboratory air as obtained with the L system for $N = 1$, 19, and 31 ion passages through the MTOF-MS. As one can see the 0.011 u mass doublet of CO–N_2 is barely resolved for $N = 1$. However it is well resolved for $N = 19$ and for $N = 31$.

From such mass measurements we determined the mass resolving power $R(N) = m/\Delta m$ as function of N which resulted in an approximately linear increase in $R(N)$ with N as is illustrated in Fig. 5. From this linear increase one can conclude that the condition of energy isochronicity is fulfilled at least approximately for all investigated N values. Since each achieved $R(N)$ value is the result of a special adjustment of several potentials of the MTOF-MS the observed fluctuation in $R(N)$ is probably due to a sometimes better and sometimes not so good experimental parameter optimization.

Comparing the three parts of Fig. 4 one notices an unsymmetric peak broadening increases considerably with the N. This peak broadening is a consequence of image aberrations of second order which probably can be reduced by a better optimization of the electrode arrangement in the MTOF-MS.

The transmission $T(N)$ through the MTOF-MS was recorded together with $R(N)$ for different N values. This dependence we demonstrate by plotting in Fig. 6 the relative transmission $T(N)/T(1)$ as a function of N, where $T(1)$ is the single-pass transmission. This $T(N)/T(1)$ dropped ≈50% when going from $N = 1$ to $N = 3$, while for more than 3 passages transmission losses of ≈5% per passage were observed. For 31 passages we thus observed an overall transmission of ≈25%. The first 50% loss shows that the lens strengths, found to be optimal for the multipass operation allowed only a smaller acceptance of the system than the acceptance found for the optimal choice of lens strengths for the single-pass operation. For the ≈5% loss per passage, however, we have no well grounded explanation. We can only assume that either our alignment is still not perfect enough or that the beam halo due to lateral aberrations grows in reality more than our theory predicts.

At this time the performance of our MTOF-MS is limited by image aberrations and by the stability of the power supplies for the electrodes. Both these

limitations, however, we should be able to reduce, so that mass resolving powers of $\approx 10^5$ should be reachable eventually.

Acknowledgements

For financial support the authors are grateful to the German Ministry for "Bildung und Forschung" as well as to the Max-Planck-Institut fur Aeronomie in Lindau.

References

[1] H. Wollnik, Optics of Charged Particles, Academic, Orlando, FL, 1987.
[2] B. Franzke, Nucl. Instrum. Methods, Phys. Res. B 24/25 (1987) 18.
[3] H. Wollnik, K. Beckert, T. Beha, F. Bosch, H. Eickhoff, B. Franzke, Y. Fujita, H. Geissel, M. Hausmann, H. Irnich, H.C. Jung, Th. Kerscher, O. Klepper, H.J. Kluge, C. Kozhuharov, G. Kraus, K.E.G. Löbner, G. Munzenberg, F. Nickel, F. Nolden, Y. Novikov, T. Radon, H. Reich, C. Scheidenberger, B. Schlitt, W. Schwab, A. Schwinn, M. Steck, K. Sümmerer, Nucl. Phys. A 616 (1997) 346.
[4] W.P. Poschenrieder, Int. J. Mass Spectrom. Ion Processes 9 (1972) 35.
[5] H. Wollnik, Nucl. Instrum. Methods, Phys. Res. A 258/25 (1987) 289.
[6] H. Wollnik, Int. J. Mass Spectrom. Ion Processes 131 (1994) 387.
[7] H. Wollnik, in Mass Spectrometry in Biomolecular Sciences, R.M. Caprioli (Ed.), 1996, Kluwer, Dordrecht, 1996, p. 111.
[8] H. Wollnik, in Nuclear Structure, C. Baktash (Ed.), AIP, New York, 1999, Vol. 481, p. 107.
[9] M. Toyoda, M. Ishihara, S. Yamaguchi, H. Ito, T. Matsuo, R. Roll, H. Rosenbauer, J. Mass Spectrom. 35 (2000) 163.
[10] M. Hausmann, K. Beckert, F. Bosch, A. Dolinskiy, H. Eickhoff, M. Falch, B. Franczak, B. Franzke, H. Geissel, Th. Kerscher, O. Klepper, H.H. Kluge, C. Kozhuharov, K.E.G. Lobner, G. Munzenberg, F. Nolden, Y. Novikov, H. Schatz, C. Scheidenberger, J. Stadlmann, M. Steck, T. Winkler, H. Wollnik, Nucl. Instrum. Methods, Phys. Res. A, 446 (2000) 569.
[11] H. Wollnik, M. Przewloka, Int. J. Mass Spectrom. Ion Processes 96 (1990) 267.
[12] A. Casares, A. Kholomeev, N. Nankov, R. Roll, H. Rosenbauer, H. Wollnik, Proceedings of the 47th ASMS Conference on Mass Spectrometry, Dallas, TX, 1999.
[13] W. Plass, thesis, Giessen, (1997).
[14] R. Grix, U. Grüner, G. Li, H. Stroh, H. Wollnik, Int. J. Mass Spectrom. Ion Processes 93 (1998) 323.
[15] C.K.G. Piyadasa, P. Haakenson, T.R. Ariyaratne, Rapid Commun. Mass Spectrom. 13 (1999) 620.